Global J. Environ. Sci. Manage. 8(3): 339-352, Summer 2022, Serial #31

Global Journal of Environmental Science and Management
(GJESM)

Homepage: https://www.gjesm.net/

ORIGINAL RESEARCH PAPER

Flood hazard simulation and mapping using digital elevation models with different resolutions

G.R. Puno[1,*], R.C.C. Puno[2], I.V. Maghuyop[2]

[1]*Department of Forest Resources Management, College of Forestry and Environmental Science, Central Mindanao University, Musuan, Maramag, Bukidnon, Philippines*

[2]*Department of Environmental Science, College of Forestry and Environmental Science, Central Mindanao University, Musuan, Maramag, Bukidnon, Philippines*

ARTICLE INFO

Article History:
Received 04 September 2021
Revised 09 November 2021
Accepted 14 January 2022

Keywords:
Bathymetry
Calibration
Floodplain
Remote sensing
Two-dimensional map

ABSTRACT

BACKGROUND AND OBJECTIVES: Fine topographic information is a key input parameter for a detailed flood simulation and mapping. This study aimed to compare the accuracy statistics of the flood models developed using the digital elevation datasets with different resolutions from the light detection and ranging and interferometric synthetic aperture radar systems.

METHODS: The study applied the Hydrologic Engineering Center-Hydrologic Modeling System and Hydrologic Engineering Center-River Analysis System models workable within the geographic information system to simulate and map flood hazards in Maapag Watershed. The models' validity and accuracy were tested using the confusion error matrix, f-measurement, and the root means square error statistics.

FINDINGS: Results show that using the light detection and ranging dataset, the model is accurate at 88%, 0.61, and 0.41; while using the interferometric synthetic aperture radar dataset, the model is accurate at 76%, 0.34, 0.53; for the error matrix, f-measurement, and root mean square error; respectively.

CONCLUSION: The model developed using the light detection and ranging dataset showed higher accuracy than the model developed using the interferometric synthetic aperture radar. Nevertheless, the latter can be used for flood simulation and mapping as an alternative to the former considering the cost of model implementation and the smaller degree of accuracy residual error. Hence, flood modelers particularly from local authorities prefer to use coarser datasets to optimize the budget for flood simulation and mapping undertakings.

DOI: 10.22034/gjesm.2022.03.04

NUMBER OF REFERENCES	NUMBER OF FIGURES	NUMBER OF TABLES
39	5	3

*Corresponding Author:
Email: *grpuno@cmu.edu.ph*
Phone: +9166 918 259
ORCID: 0000-0002-7170-641X

Note: Discussion period for this manuscript open until October 1, 2022 on GJESM website at the "Show Article".

INTRODUCTION

Food hazard research has since been important in the last two decades and continues to be relevant in future climate scenarios to develop realistic solutions to disaster risk problems (Pinos and Quesada-Roman, 2022). For more detailed and accurate outputs, studies on flood hazards are conducted through simulations using high-resolution digital elevation models (DEMs) such as those derived from the light detection and ranging (LiDAR) and interferometric synthetic aperture radar (IfSAR) systems. DEM, as a representation of the natural and man-altered ground surface, is valid for any three-dimensional and topographic visualization. It is excellent as an input dataset in flood modeling and simulation for risk management strategies (Li *et al.,* 2017; Guidolin *et al.,* 2016). High-resolution DEM is sought in flood hazard modeling studies to give a quality result as it determines specific areas where inundation might occur in the particular watershed (Alivio *et al.,* 2019; Hawker *et al.,* 2018). Highly detailed DEMs are the most preferable datasets in hydrologic modeling and simulations where accurate flood hazard maps are sought. Appropriate DEM specification is an essential factor to enhance flood simulation accuracy and reliability. Enhanced simulations reliability is important in generating detailed information that contributes to the cost-effective approaches in the reduction and prevention of damages and economic losses caused by flood hazards (Demir and Kisi, 2016). Two of the fastest-growing remote sensing technologies that provide satisfactory resolution DEMs are light detection and ranging (LiDAR) and interferometric synthetic aperture radar (IfSAR) (Hawker *et al.,* 2018). LiDAR and the IfSAR systems offer high-resolution DEMS suitable for developing hydrologic models with more refined and accurate model outputs. Theoretically, LiDAR DEM offers more advantages than IfSAR DEM as it provides a flood hazard map with more detailed and precise information. Airborne LiDAR is also an emerging remote sensing state-of-the-art system design, technology and application (Li *et al.,* 2020). LiDAR is capable of providing highly accurate spatial data and information widely used for hazard assessment, disaster risk assessment and flood modeling. The advancement of LiDAR technology systems facilitated and improved flood applications (Muhadi *et al*., 2020). It is the most useful elevation dataset for mapping small regions with high accuracy. However, acquiring LiDAR DEM is costly especially for large-area applications. Thus, LiDAR data is limited in areas with wider coverage due to expensive acquisition operations (Khalid *et al*., 2016). High acquisition cost is a hindrance in using LiDAR datasets in some developing countries (Muhadi *et al*., 2020). IfSAR, also termed InSAR, on the other hand, is considered a relatively cheaper and complementary 3-D mapping technology with varying applications in many fields including flood simulations and mapping flood hazards (Lu *et al*., 2007). It is more cost-effective compared to LiDAR and is readily available for use in flood modeling with quality and accuracy of results higher than other satellite systems (Gopal, 2010). Nevertheless, LiDAR is generally the most preferred technology for deriving DEM despite its high cost (Hashim *et al*., 2014). In a disaster-prone country like the Philippines, billions worth of local funds had been allocated for research projects on flood hazard management particularly mapping and monitoring in some priority river basins using LiDAR technologies. The project allocated the highest bulk of the cost for the acquisition of LiDAR datasets (Mateo, 2013; Ronda, 2013). Meanwhile, the government has also acquired IfSAR DEM which covers the whole country (Belen, 2015). The desire for effective flood hazard maps at the onslaught of disaster in recent years instigated the use of high-resolution DEMs from LiDAR and IfSAR technologies for flood modeling and simulation studies (Talisay *et al*., 2019). The accuracy of the results in such studies is generally acceptable due to the good topographic representation of both DEMs. However, LiDAR is still more preferred than other digital elevation datasets as it provides higher flood simulation accuracy with minimal errors (Ogania *et al*., 2019). But still, in any project requirements and resources, the cost and economic feasibility perpetually remain the critical factors (Chen and Hill, 2007). Previous studies on the comparison of LiDAR and IfSAR datasets on flood simulations focus only on the predictive accuracy and precision of the model without expounding the degree of difference and the economic considerations. The computer application software used in the study includes the Hydrologic Engineering Center-Hydrologic Modeling System (HEC-HMS) and the Hydrologic Engineering Center-River Analysis System (HEC-RAS) models of the U.S. Army Corps of Engineers (USACE, 1964).

HEC-HMS and HEC-RAS models are workable within the geographic information systems (GIS) environment with HEC-GeoHMS and HEC-GeoRAS as their geospatial extension, respectively. The developed cost-sensitive model with acceptable accuracy performance is essential to enhance the management capability of pertinent government and non-government organizations in implementing the programs and projects regarding urban flood risk reduction and management both at the national and local levels. This study aimed to compare the accuracy statistics of the flood models developed using the digital elevation datasets with different resolutions from the light detection and ranging and interferometric synthetic aperture radar systems. Furthermore, this study aimed to investigate the applicability of IfSAR DEM as an alternative to LiDAR DEM based on the residual error of accuracies of the two models using the three statistical tests, namely the confusion error matrix, f-measurement, and the root mean square error (RMSE). By doing so, this study generates information helpful in formulating a science-based and cost-sensitive policy statement specific to the application of appropriate datasets for flood simulation and mapping necessary in the economically-sound implementation of disaster risk mitigation and management. This study was conducted in the Maapag Watershed, Valencia City, Bukidnon, Philippines from 2017 to 2019.

MATERIALS AND METHODS

Study watershed

This study covered the Maapag Watershed with geographical coordinates of 7° 45' 55.77" to 7° 56' 10.27" north and 125° 4' 40.03" to 125° 16' 25.51" east. The watershed extends at a width of 15 km and a length of 16.80 km with approximately 251.20 km^2. The majority of the watershed area falls under the jurisdiction of Valencia City, Bukidnon, Mindanao, Philippines (Fig. 1). Some tributaries, specifically the southern portion of the watershed, fall within the Municipality of Quezon, Bukidnon. Maapag Watershed drains to Mindanao River Basin, the second largest river basin in the country. The vast expanse of the Maapag floodplain is dominantly cultivated for rice production and for settlement areas that are regularly flooded, especially during heavy rainfalls with waters coming from the upstream terrains. Most often, the local government authorities warn the communities within the floodplain to be prepared during heavy rain to mitigate the negative impacts of flood hazards on human lives and properties (Cantal-Albasin, 2017).

DEM description

DEM is a computer graphic representation of elevation data in three-dimensional coordinates

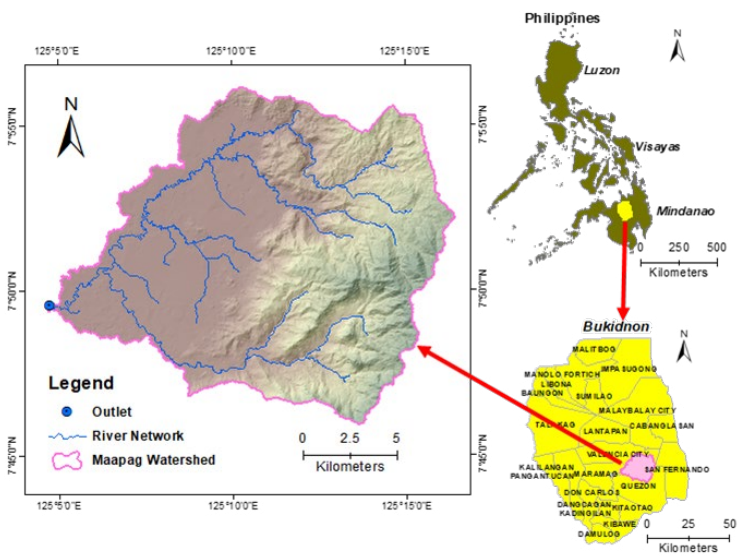

Fig. 1: Geographic location of the study area in Maapag Watershed, Valencia City of Bukidnon, Mindanao, Philippines

usually used in geographic information systems to visualize the terrain of the ground surface (Gandhi and Sarkar, 2016). Acquiring the DEMs can be done through photogrammetry like the LiDAR and IfSAR technologies. LiDAR technique uses airborne sensors emitting lasers to the Earth deriving DEM with a resolution of 1 m. The produced DEM has a vertical accuracy ranging from ±5 to 15 cm and horizontal accuracy of less than 1 m (Wedajo, 2017). The uses of LiDAR enable grain-scale surface roughness and provide highly accurate ground and urban landscape topographic datasets, which are essential characteristics for efficient simulation of the flood (Puno *et al*., 2019). In the Philippines, the LiDAR data was made available through the Data Acquisition Component (DAC) of the University of the Philippines-Disaster Risk and Exposure Assessment for Mitigation (UP-DREAM) and Phil-LiDAR Programs of the UP Training Center for Applied Geodesy and Photogrammetry (UP-TCAGP) supported by the Department of Science and Technology (DOST) (Makinano-Santillan *et al*., 2019). On the other hand, the IfSAR technology utilizes a Synthetic Aperture Radar (SAR) system of two or more images of the same extracted area (Lu *et al*., 2007). The data is formed from two radar images of the recorded phase and amplitude using microwave echoes, a combination of conventional SAR and interferometry techniques (Smith, 2002). The interaction of electromagnetic waves measures the precise distance between satellite antenna and ground resolution elements, deriving landscape topography of subtle elevation changes (Lu *et al*., 2007). The available IfSAR data in the Philippines from the National Mapping and Resource Information Authority (NAMRIA) has a resolution of 5 m with 1 m RMSE vertical accuracy and 2 m RMSE horizontal accuracy (Belen, 2015). Table 1 presents the comparison of the two digital elevation models used in the study.

DEM processing and preparation

Activities for DEM processing followed the workflows within the GIS environment involving data editing, mosaicking, calibration, and bathymetric data burning. The LiDAR datasets from the DREAM and Phil-LiDAR Programs were available in a form of spatial coordinates in American standard code for information interchange (ASCII) format file and drawing exchange format (DXF). ArcTeam toolbar developed by the UP Diliman Data Processing Component was utilized in generating DEM formats, particularly in the form of a digital terrain model (DTM). DEM editing included filling data gaps in the flight mission with no data using the FillDataGaps toolbar. The process also involved interpolation and object retrieval techniques to edit the DEM by omitting unnecessary objects in the DTM, ensuring unobstructed water flow in river systems, and filling of missed portions using a secondary DTM layer. These two processes served as the cleaning and refining of DTM. Adjacent edited flight missions were then mosaicked with edges smoothened. DTMs calibration was done through actual field surveys using ground validation points reckoned from mean sea level (MSL) gathered from the survey. The team conducted a resampling of the initially 5-meter resolution IfSAR DEM into 1 m and edited it following similar processes as that of LiDAR DEM. Scrutinizing the processed and mosaicked DTMs was also done for quality checking. The method also involved bathymetric data burning to integrate river morphology to DTM. This process fills the gaps created from LiDAR due to the inability of its laser pulse to penetrate the water surface and the inaccurate river bed elevations data from IfSAR. Conducting the bathymetric survey to acquire the desired data involves the collection of actual heights and coordinate points and the river geometry using the high-precision global navigation satellite system (GNSS) instrument applied with real-time kinematic

Table 1: Comparison of the two digital elevation models

Descriptions	LiDAR	IfSAR
Radar systems	Airborne	Airborne/Spaceborne
Vertical accuracy	<0.15 m	1 m
Horizontal accuracy	< 1 m	2 m
Resolution/pixel size	1 m	5 m
Model	DTM/DSM	DTM/DSM
Availability	Upon request	Upon request
Source	UP-DREAM	NAMRIA

(RTK) techniques. The process enabled the generation of a new raster using the inverse distance weighted (IDW) interpolation method of the Spatial Analyst tool of ArcGIS 10.2.2 version.

Basin model development, calibration and evaluation

The hydrologic models applied in this flood modeling and simulation studies are the HEC-HMS and HEC-RAS of the US Army Corps of Engineers. HEC-HMS was utilized to simulate the hydrologic processes while HEC-RAS was for the simulation of two-dimensional unsteady flow hydraulic analysis (Santillan and Makinano-Santillan, 2016). Both are open-source computer programs extensively utilized in modeling researches and studies involving hydrological processes (Divin and Mikita, 2016). The study team developed the hydrologic basin model of Maapag Watershed using the HEC-GeoHMS extension of ArcGIS 10.2.2. Within the HEC-HMS version 3.5 workflows, the team calibrated the Maapag basin model using the actual event data collected on November 20-22, 2017, caused by the tail-end of a cold front and northeast monsoon. Calibration of the model involved manual adjustment and fine-tuning of parameters such as the soil and land cover through the "trial and error" method to fit the simulated values to the observed hydrograph. Model performance to simulate flooding events was evaluated by calculating the efficiency criteria such as the root mean square error (*RMSE*) to the standard deviation (*STDEV*) of measured data ratio (*RSR*), Nash-Sutcliffe efficiency (*NSE*), and percent bias (*PBIAS*) statistics. The *RSR* values range from 0 which indicates a perfect prediction or zero *RMSE* to a large positive value. It follows the lower *RSR*, the lower the *RMSE*, the optimal or better the model simulation performance. *RSR* is computed using Eq. 1. (Moriasi *et al*., 2007).

$$RSR = \frac{RMSE}{STDEV_O} = \frac{\sqrt{\sum_{i=1}^{n}\left(Y_i^o - Y_i^s\right)^2}}{\sqrt{\sum_{i=1}^{n}\left(Y_i^o - Y^m\right)^2}}, \quad (1)$$

where *RMSE* is the root mean square error to the standard deviation of the observed data ($STDEV_o$) ratio (*RSR*), where Y_i^o is the i^{th} observation for the evaluated variable, Y_i^s is the i^{th} simulated value for the evaluated variable, Y^m is the mean of observed data for the evaluated variable, and *n* is the total number of observations. *NSE*, on the other hand, is a test of model performance that indicates how well the plot of observed versus simulated data fits the 1:1 line. Values between 0.0 and 1.0 are generally viewed as acceptable levels of performance, whereas values <0.0 indicate an unacceptable model performance. Following the same symbols used in Eq. 1, NSE is computed using Eq. 2 (Moriasi *et al*., 2007).

$$NSE = 1 - \frac{\sum_{i=1}^{n}\left(Y_i^o - Y_i^s\right)^2}{\sum_{i=1}^{n}\left(Y_i^o - Y^m\right)^2}, \quad (2)$$

PBIA is another test of model performance that assesses the average tendency of the predicted results to overestimate or underestimate the field observed data. A PBIAS of 0.0 indicates an accurate model performance. A positive and negative PBIAS value indicates underestimation and overestimation, respectively. With the same symbols used from the previous equations, PBIAS is calculated using Eq. 3 (Moriasi *et al*., 2007).

$$PBIAS = \frac{\sum_{i=1}^{n}\left(Y_i^o - Y_i^s\right)}{\sum_{i=1}^{n} Y_i^o} 100 \quad (3)$$

With acceptable statistical results, the calibrated and evaluated model of Maapag enabled simulation of flood depth and extent covering the floodplain of the river basin using the rainfall data from the tropical storm on December 21-23, 2017.

Flood simulation

For the hydraulic simulation, the team established the model using the HEC-GeoRAS extension tool in ArcGIS 10.2.2. The team also prepared the following datasets as the 2-dimensional (2D) area; land use/ land cover (LULC) map with incorporated Manning's *n* values; break lines shapefile of roads, riverbanks and the sudden change of elevation; and terrain data of LiDAR and IfSAR. A discharge hydrograph of the tropical storm simulated by the calibrated model was used for the unsteady flow analysis of hydraulic simulation. Flow data were inputted in each boundary condition identified as points for discharge inflows. A constant value of 0.01 was assigned for the standard depth and the outlet of the 2D domain area. Precipitation data from the calibrated HMS for

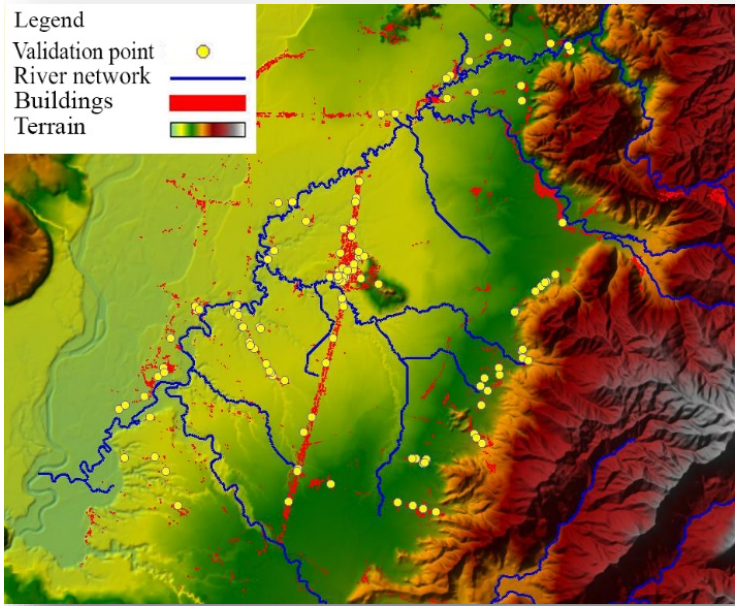

Fig. 2: Validation points in the floodplain of the watershed

the same event was added as an additional boundary condition covering the whole 2D domain area extent. Two separate unsteady flow analyses using the LiDAR and IfSAR DEMs were consequently performed in HEC-RAS version 5.0.

Flood validation

Around 120 points randomly scattered in the floodplain of Maapag were established for flood validation (Fig. 2). Each point represents a random household in the floodplain as determined by the extracted building features using the LiDAR-derived digital surface model (DSM), which portrays above-surface features such as buildings (Sharma *et al*., 2010). Flood information consisting of flood height, flood duration, and other relevant information were collected from each point through personal interviews. These points were then loaded in ArcGIS and plotted against the simulated flood depths using the LiDAR and IfSAR DEMs.

Three statistical tests, namely the error matrix or accuracy, f-measurement, and root mean square error, were run to measure the accuracy and validity of the simulated flood using the two DEMs. These statistical metrics are the common standard procedures for determining the similarity of maps in various mapping and model performance evaluation studies (Timbadiya *et al*., 2011). The accuracy statistic of the simulated flood depths was computed using Eq. 4 (Cabrera and Lee, 2019).

$$Accuracy\% = \frac{(A+B)}{N} \tag{4}$$

where *A* is the number of correctly predicted flooded points, *B* is the number of correctly predicted not flooded points, and *N* is the total number of collected points. The f-measurement was computed using Eq. 5 (Jung *et al*., 2014).

$$F = \frac{A}{(A+B+C)} \tag{5}$$

where *A* is the same as described in equation 4, *B* is the number of points predicted by the model as flooded but not flooded in reality, and *C* is the number of points that are predicted by the model as not flooded but flooded in reality. The RMSE statistics for models' validity and reliability test were computed using Eq. 6 (Timbadiya *et al*., 2011).

$$RMSE = \sqrt{\frac{\sum_{i=1}^{n}(X_{mo} - X_o)^2}{n}} \tag{6}$$

where X_{mo} is the modeled values, X_o is the observed

values at a time/place *i*., *n* is the number of points.

Flood exposure analysis

This process quantifies the number of exposed buildings based on two simulated flood hazards developed using LiDAR and IfSAR DEMs, respectively. The initial process involved the extraction of building features from LiDAR DSM. Determining the number of exposed buildings was done through superimposing separately the building features map layers with the flood hazard maps derived from the simulation models using LiDAR and IfSAR datasets.

RESULTS AND DISCUSSION

Processed DEMs

Fig. 3 illustrates the processed DEMs of the 1 meter-resolution, LiDAR, and 5 meter-resolution, IfSAR, integrated with bathymetric data. A more detailed DEM, as characterized by smaller stream networks, is evident in the LiDAR DEM. This observation confirmed the findings from previous studies where LiDAR DEM is capable of offering detailed elevation data that can be used to improve flood-model input and consequently increase the accuracy of the flood modeling results (Leitao and de Sousa, 2018). Meanwhile, IfSAR DEM appears more coarse and is unable to capture other tributary streams. Moreover, the two DEMs have a minimal difference when it comes to elevation ranges. The 2D area boundary of the two DEMs, which sets the extent of simulation, has the same highest elevation of 992 m. On the other hand, the lowest elevation is 275 m and 283 m for LiDAR and IfSAR DEMs, respectively.

Hydrologic basin model

The delineation of the basin boundary along with the river network or reaches was accomplished during basin model preparation using the HEC-GeoHMS extension tool. Calibrating the HMS model involved fitting the simulated discharge with the observed discharge hydrograph. Calibration was through manual adjustment of parameters and visual evaluation of the fitted lines of the observed and simulated values in the hydrographs. After closely fitting the hydrographs, model performance was subsequently evaluated using the validation guidelines of Moriasi *et al*. (2007). The initial result of evaluation before calibration showed acceptable model performance considered as „good" for both RSR and NSE and „satisfactory" for PBIAS. After calibration, the model performance result shows „very good" for the three statistical tests. Fig. 4 shows the observed hydrograph against the calibrated and

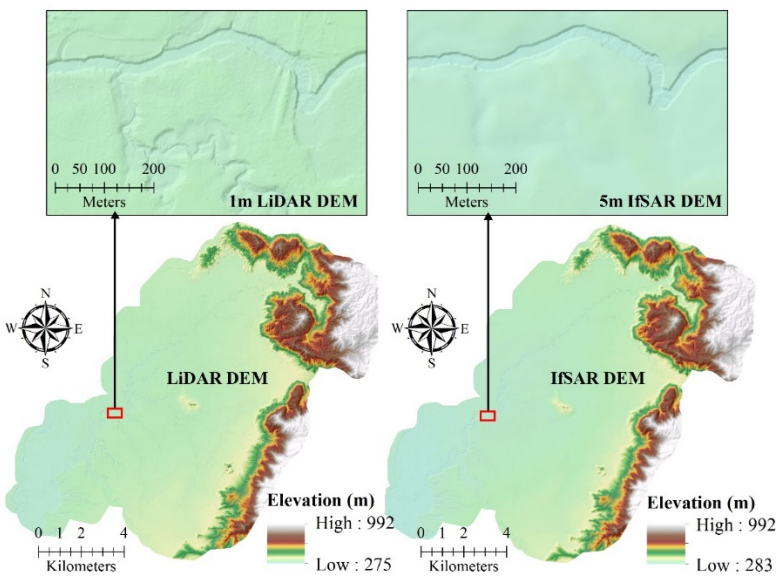

Fig. 3: Processed LiDAR and IfSAR DEMs

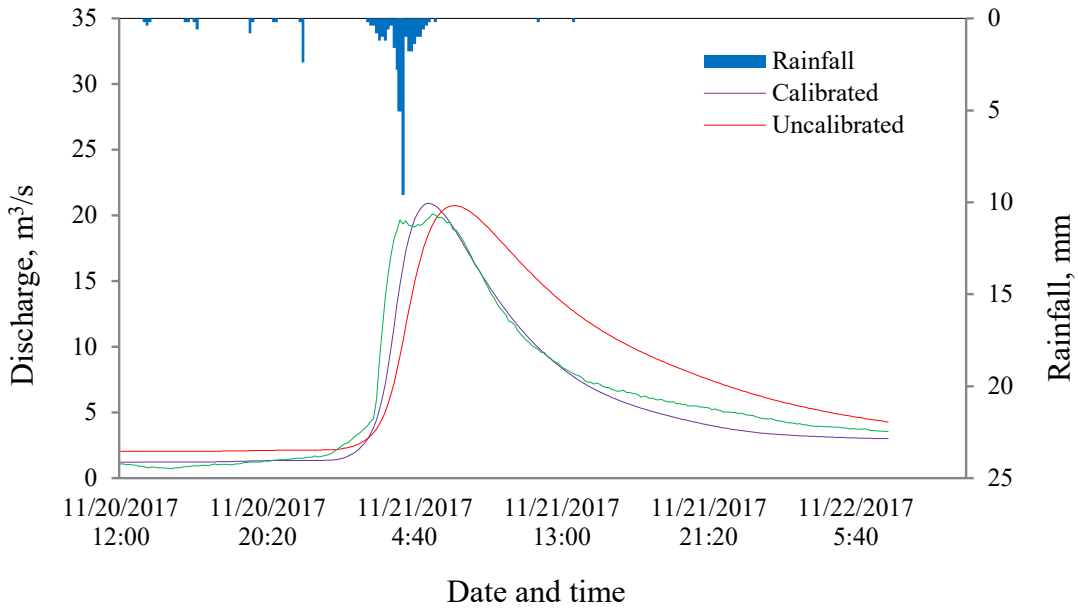

Fig. 4: Calibrated and uncalibrated simulated hydrographs against actual discharge

Table 2: Statistical analysis of model performance

Statistical matrices	Pre-calibration		Post calibration	
	Value	Remarks	Value	Remarks
RSR	0.56	Good	0.23	Very Good
NSE	0.68	Good	0.95	Very Good
PBIAS	-22.39	Satisfactory	8.61	Very Good

uncalibrated simulated hydrographs, while Table 2 shows the statistical model performance before and after calibration. The calibrated model was used to reconstruct the flood event that occurred last December 21-23, 2017.

Flood simulation and mapping

The geometric data consists of a 2D domain area that determines the simulation extent with model boundary conditions corresponding to the baseflow depth, precipitation boundary, and the flow hydrograph conditions which contained the simulated discharge data of the calibrated HMS model. Fig. 5 depicts the result of the simulated flood using the 5 m IfSAR and 1 m LiDAR DEM with the terrain models overlaid with extracted features of building structures from LiDAR DSM. A closer look reveals that the differences in topographic details resulted in varying flood propagation in both IfSAR and LiDAR simulations. Moreover, the model developed with IfSAR has recognizable clamped inundations due to the less intricate of smaller tributaries. It was also unable to capture the inundated channels and its floodplain, which are barely flooded, unlike LiDAR DEM-based simulation. Comparatively, LiDAR and IFSAR DEMs yielded the simulated flood areas of 35.82 km^2 and 35.59 km^2, respectively, showing a slight difference of 0.23 km^2. The LiDAR-based simulation has wider inundation which may be due to a broader extent of the flat terrain of lower elevations occupied by floodwaters. Varying observations were noted in some related studies. Chen and Hill (2007) concluded that due to the relatively smooth terrain of coarser DEM, there are few terrain details restraining water dispersion and reducing the area of inundation. In contrast, Md Ali *et al*. (2015),

observed a wider flood extent in DEM with coarser resolution. Simulation using LiDAR and IfSAR DEMS revealed different maximum flood depths of 23.66 m and 19.54 m, respectively. As reported, flood model simulation results show differences in water depths and inundation when using detailed DEMs (Muhadi *et al*., 2020). Furthermore, in comparing the two flood simulations of different DEMs, the building features had not accurately occupied the actual locations, particularly with IfSAR DEM compared to LiDAR DEM. Such observation is expected since exposure datasets which consist of building structures, were extracted from LiDAR DSM only.

Flood validation and accuracy

Information on the historic flood experiences included the 120 locations within the 2D domain flood simulation area. Each point represented by a household is either flooded or not flooded during the event. Flood height was measured in each flooded point. Following the spatial analyst tool of ArcGIS workflow, the simulated flood depths using the two DEMs were extracted and the outputs of which were used to calculate the accuracy metrics. Table 3 shows the validation results of the simulated flood event using the three accuracy metrics.

Comparing the two flood models developed with LiDAR and IfSAR DEM datasets using the error matrix approach, the former yielded a more accurate result with a difference of 12% accuracy. Error matrix is influenced by the number of correctly predicted flooded and not-flooded points by the model simulation and is interpreted as the overall reliability (Cabrera and Lee, 2019). For both simulations, the number of correctly predicted flooded and not-flood points is greater than the incorrectly predicted points. Simulation using LiDAR DEM mainly attained a high percentage which passed the acceptable value of 85% for the overall accuracy as reported by Foody (2008). On the other hand, the simulation using IfSAR failed to satisfy the acceptable prescribed percentage overall accuracy. Test of accuracy using f-measurement revealed an intermediate fit for the simulation using LiDAR and a bad fit for the model using IfSAR. Based on Breilh *et al*. (2013), flood simulated using LiDAR DEM is

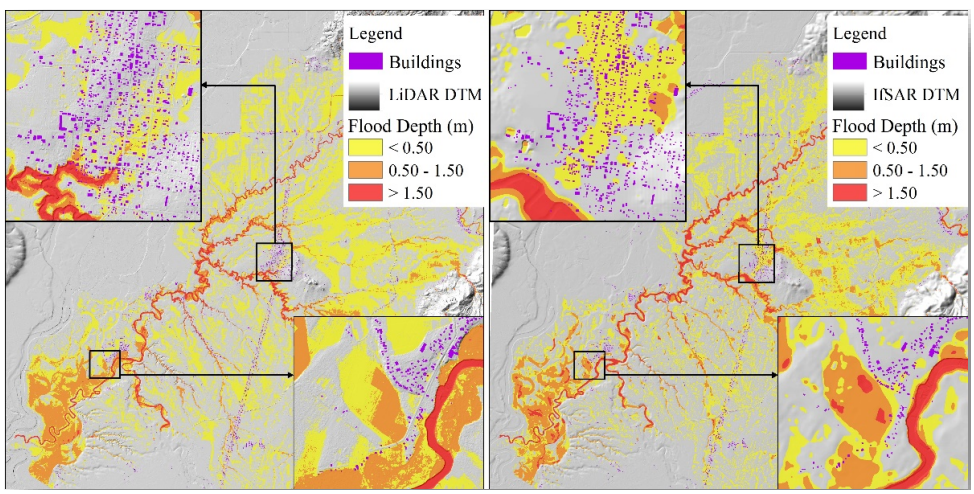

Fig. 5: Simulated flood using LiDAR and IfSAR DEMs

Table 3: Accuracy tests of flood simulation models using LiDAR and IfSAR DEMs

Accuracy metrics	LiDAR DEM-based model	IfSAR DEM-based model
Error Matrix	88%	76%
F-measurement	0.61	0.34
RMSE	0.41	0.53

acceptable after attaining an f-measure of above 0.5. This accuracy metric reveals that several incorrectly predicted flooded and not flooded points are few for the model using LiDAR but too numerous for the simulation using IfSAR. Comparatively, the IfSAR simulation showed an overestimation of flooding than the LiDAR DEM simulation. The RMSE metric explains the differences between the predicted and observed data, with the significant errors affecting the rating (Najafi and Salam, 2016). The test showed a low RMSE for LiDAR simulation but high RMSE for IfSAR. Specifically, the simulation using IfSAR DEM has a more significant error compared to LiDAR DEM as indicated by the higher RMSE value. Between the two, the flood model using LiDAR falls within the acceptable level of RMSE, which is below 0.5. Coarser DEM contains more errors in elevation which tend to overestimate hazard levels and underestimate flooded areas. Overall, the LIDAR DEM-based flood model has statistically yielded a better result than IfSAR DEM-based model. However, LiDAR data has some issues that need to be addressed regarding filtering processes and data density resulting in a longer computational time to simulate flood models (Muhadi, *et al*., 2020). Besides, the high cost of LiDAR data acquisition has been a constraint for its availability and operational use (Hudak *et al.,* 2011). Thus, the application of IfSAR DEM in flood modeling studies is still preferred (Mokhtar *et al*., 2018).

Flood exposure analysis

This analysis allows the calculation of the building features exposed to risk according to the simulated flood using the two kinds of DEMs categorized into three hazard levels namely „low", „medium", and „high" with flood depth of <0.5 m, 0.5-1.5 m, and >1.5 m, respectively. For both simulations, the majority of the flooded buildings were under the „low" hazard level, followed by „medium" and the „high". The IfSAR-based simulation consistently showed a lower number of flooded buildings under the „low" and „medium" hazard category levels. In LiDAR-based simulation, the total number of flooded buildings is 3580 (38%) of the total buildings in the floodplain. On the other hand, the IfSAR simulation inundates a total of 2896 (30%) buildings. A difference of 684 or 8% more flooded building features, the majority of which are residential, were extracted using the LiDAR-based flood hazard maps. In the aspect of disaster operations and management, there is an underestimation of flooded buildings using IfSAR. This generated information is necessary as it serves as a basis for making an optimal decision on the exact location and coverage of hazards in the localities that need immediate rescue and response operations during flood disasters.

CONCLUSION

The flood simulation model using LiDAR DEM passed the three statistics of accuracy tests showing more precise results. The simulated flood using IfSAR DEM yielded near to acceptable results but failed to statistically satisfy the overall prescribed accuracy tests. Flood simulation shows differences in flood depth with LiDAR DEM-based model having the deeper inundation indicating more detailed results. In the infrastructure feature extraction, both models showed similar trends where the majority of the flooded buildings were under the low hazard level indicating the applicability of both DEMs in the process. Generally, the LiDAR DEM dataset revealed to be advantageous than IfSAR DEM and is more appropriate when it comes to the accurate estimation of flood impacts up to the household level. However, difficulty in terms of data storage that results in a longer processing time to simulate flood models is one of its drawbacks. Additionally, the cost of LiDAR DEM data acquisition is relatively high. An agency or the local government units may limit the coverage to focus on the highly populated areas to minimize the LiDAR data acquisition cost. Thus, in flood-prone agricultural lands where critical analysis is unnecessary, IfSAR can be used for flood simulation. Areas covered with other land uses may be represented by IfSAR and mosaicked with the available LiDAR datasets on specific floodplains. Overall, this study presents the benefit of using fine-resolution DEM such as a LiDAR over coarser DEM such as IfSAR, especially when seeking a more detailed and accurate flood model simulation. However, with the issues and concerns about LiDAR data acquisition, processing and storage, the IfSAR system is still preferred as it offers a more cost-sensitive DEM dataset for use in the process of flood simulation model development and updating which are necessary for the economically-optimal implementation of flood hazards monitoring and management.

AUTHOR CONTRIBUTIONS

G.R. Puno acted as the project leader of the study and prepared the manuscript main file, GIS and other databases, layout design, and graphs. R.C.C. Puno acted as the research associate of the project and was involved in several activities such as data collection, flood simulation, and hazard mapping, and land use/land cover map generation using satellite images. I.V. Maghuyop was involved in the manuscript preparation and editing.

ACKNOWLEDGMENTS

This study is a product of the Geo-Informatics for the systematic assessment of flood effects and risks in Northern Mindanao and Cotabato, Philippines (Geo-SAFER Northern Mindanao/Cotabato) Project No. 2, funded by the Department of Science and Technology-Philippine Council for Industry, Energy, and Emerging Technology Research and Development (DOST-PCIEERD) with a financial account [Grant number 1-416-154]; and the Provincial Government of Bukidnon with a financial account [Grant number 116-164]. The authors also acknowledge the administration of Central Mindanao University and the local government units of Valencia City for the logistics.

CONFLICT OF INTEREST

The authors declare no potential conflict of interest regarding the publication of this work. Also, the ethical issues including plagiarism, informed consent, misconduct, data fabrication and, or falsification, double publication and, or submission, and redundancy have been completely witnessed by the authors.

OPEN ACCESS

PUBLISHER'S NOTE

ABBREVIATIONS

%	Percent
0	Degrees
'	Minutes
"	Seconds
Σ	Summation sign
>	Greater than
<	Less than
2D	Two-dimensional
A	Number of correctly predicted flooded points
ArcGIS	Geographic information system software product
ASCII	American standard code for information interchange
B	Number of correctly predicted not flooded points
C	Number of points predicted as not flooded but flooded in reality
DAC	Data acquisition component
DEM	Digital elevation model
DOST	Department of Science and Technology
DREAM	Disaster Risk and Exposure Assessment for Mitigation
DSM	Digital surface model
DTM	Digital terrain model
DXF	Drawing exchange format
Eq	Equation
F	F-measurement
Fig.	Figure

Geo-SAFER	Geo-Informatics for the Systematic Assessment of Flood Effects and Risks
GIS	Geographic information system
GNSS	Global navigation satellite system
HEC-GeoHMS	Hydrologic engineering center-hydrologic modeling system GIS interface
HEC-GeoRAS	Hydrologic engineering center-river analysis system GIS interface
HEC-HMS	Hydrologic engineering center-hydrologic modeling system
HEC-RAS	Hydrologic engineering center-river analysis system
IDW	Inverse distance weighted
IfSAR	Interferometric synthetic aperture radar
i^{th}	Ith number
km	kilometer
Km^2	Kilometer squared
LiDAR	Light detection and ranging
LULC	Land use or land cover
m	Meter
mm	Millimeter
m^3/s	Cubic meter per second
MSL	Mean sea level
n	Total number of observations
N	Total number of collected points
n	Number of points
NAMRIA	National Mapping and Resource Information Authority
PBIAS	Percent bias
PCIEERD	Philippine Council for Industry, Energy, and Emerging Technology Research and Development
Phil-LiDAR	Philippine-Light Detection and Ranging
RMSE	Root mean square error
RSR	RMSE-observation standard deviation ratio
RTK	Real-time kinematic
SAR	Synthetic aperture radar
$STDEV_o$	The standard deviation of the observed data
UP	University of the Philippines
TCAGP	Training Center for Applied Geodesy and Photogrammetry
US	United States
USACE	United States Army Corps of Engineers
X_{mo}	Modeled values
X_o	Observed values
Y^m	Mean of the observed value of the evaluated variable
Y^o	Observed value of the evaluated variable
Y^s	Simulated value of the evaluated variable

REFERENCES

Alivio, M.B.T.; Puno, G.R.; Talisay, B.A.M., (2019). Flood hazard zones using 2d hydrodynamic modeling and remote sensing approaches. Global J. Environ. Sci. Manage., 5(1): 1-16 (**16 pages**).http://dx.doi.org/10.22034/gjesm.2019.01.01

Belen, R.D.M., (2015). Mapping of the typhoon Haiyan affected areas in the Philippines using geospatial data and very high-resolution satellite images. In 20th United Nations Regional Cartographic Conference for Asia and the Pacific. Jeju, Islands, 6-9 October.

Breilh, J.F.; Chaumillon, E.; Bertin, X.; Gravelle, M., (2013). Assessment of static flood modeling techniques: Application to contrasting marshes flooded during Xynthia (western France). Nat. Nat. Hazards Earth Syst. Sci., 13(6): 1595-1612 (**18 pages**).

Cabrera, J.S.; Lee, H.S., (2019). Flood-prone area assessment using GIS-based multi-criteria analysis: A case study in Davao Oriental, Philippines. Water, 11(11): 1-23 (**23 pages**).

Cantal-Albasin, G., (2017). Valencia City under state of calamity. Sun Star Philippines.

Chen, J.; Hill, A., (2007). Modeling urban flood hazard: just how much does DEM resolution matter? In Applied Geography Conferences. Indianapolis, 30: 372-379 (**8 pages**).

Demir, V.; Kisi, O., (2016). Flood hazard mapping by using geographic information system and hydraulic model: Mert River, Samsun, Turkey. Adv. Meteorol., 2677 (**9 pages**).

Divin, J.; Mikita, T., (2016). Effects of land use changes on the runoff in the landscape based on hydrological simulation in HEC-HMS and HEC-RAS using different elevation data. Acta Univ. Agric. Et Silviculturae Mendelianae Brunensis, 64(3): 759-768 (**10 pages**).

Foody, G.M., (2008). Harshness in image classification accuracy assessment. Int. J. Remote Sens., 29(11): 3137-3158 (**22 pages**).

Gandhi, S.M.; Sarkar, B.C., (2016). Essentials of Mineral Exploration and Evaluation. In: Catena, Walker and Willgossse, Digital elevation models.

Gopal, S., (2010). IFSAR: Mapping geospatial intelligence. Geospatial World.

Guidolin, M.; Chen, A.S.; Ghimire, B.; Keedwell, E.C.; Djordjevic, S.; Savic, D.A., (2016). A weighted cellular automata 2D inundation model for rapid flood analysis. Environ. Model. Software, 84: 378-394 (**17 pages**).

Hashim, S.; Naim, W.M.; Mohd, W.; Adnan, N.; Sadek Said, E.; Md Sadek, E.; Hashim, S.M.N.; Wan Mohd, W.; Md Sadek.; Á., (2014). Evaluation of vertical accuracy of airborne IFSAR and open-source digital elevation models (DEMs) for flood inundation mapping. In Regional Conference on Science, Technology and Social Sciences. Singapore, January. Springer.

Hawker, L.; Bates, P.; Neal, J.; Rougier, J., (2018). Perspectives on digital elevation model (DEM) simulation for flood modeling in the absence of a high-accuracy open access global DEM. Front. Earth Sci., 6(233): 1-9 (**9 pages**).

Hudak, A.T.; Uebler, E.H.; Falkowski, M.J., (2011). A Comparison of accuracy and cost of LiDAR versus stand exam data for landscape management on the Malheur National Forest. J. For., 109(5): 267-273 (**6 pages**).

Jung, Y.; Kim, D.; Kim, D.; Kim, M.; Lee, S.O., (2014). Simplified flood inundation mapping based on flood elevation-discharge rating curves using satellite images in gauged watersheds. Water, 6(5): 1280-1299 (**20 pages**).

Khalid, N.F.; Din, A.H.M.; Omar, K.M.; Khanan, M.F.A.; Omar, A.H.; Hamid, A.I.A.; Pa'suya, M.F., (2016). Open-source Digital Elevation Model (DEMs) Evaluation with GPS and LiDAR Data. Int. Arch. Photogramm. Remote Sens. Spatial Inf. Sci., XLII-4/W1: 299–306 (**8 pages**).

Leitao, J.P.; de Sousa, L.M., (2018). Towards the optimal fusion of high-resolution Digital Elevation Models for detailed urban flood assessment. J. Hydrol., 561: 651-661 (**11 pages**).

Li, X.; Liu·C.; Wang, Z.; Xie, X.; Li, D.; Xu, L., (2020). Airborne LiDAR: state-of-the-art of system design, technology and application. Meas. Sci. Technol., 32(3).

Li, X.; Shen, H.; Feng, R., Li, J.; Zhang, L., (2017). DEM generation from contours and a low-resolution DEM. ISPRS J. Photogramm. Remote Sens., 134(2017): 135-147 (**13 pages**).

Lu, Z.; Kwoun, O.; Rykhus, R., (2007). Interferometric synthetic aperture radar (InSAR): Its past, present and future. Photogramm. Eng. Remote Sens., 73(3): 217-221 (**5 pages**).

Makinano-Santillan, M.; Serviano, J.; Rubillos, C.K.; Amora, A.; Santillan, J.R.; Morales, E.M.; Marqueso, J.T.; Gingo, A.L., (2019). Near-real time hazard monitoring and information dissemination through integration of remote sensing, GIS, numerical modelling, web applications and social media. ISPRS Ann. Photogramm. Remote Sens. Spatial Inf. Sci., IV-3/W1: 25-32 (**8 pages**).

Mateo, J., (2013). UP allots P40M for NOAH project. Philstar Global. Philippines.

Md Ali, A.; Solomatine, D.P.; Di Badldassarre, G., (2015). Assessing the impact of different sources of topographic data on 1-D hydraulic modelling of floods. Hydrol. Earth Syst. Sci., 19(1): 631-643 (**13 pages**).

Mokhtar, E.S.; Pradhan, B.; Ghazali, A.H.; Shafri, H.Z.M., (2018). Assessing flood inundation mapping through estimated discharge using GIS and HEC-RAS model. Arab. J. Geosci., 11(682): 1-20 (**20 pages**).

Moriasi, D.N.; Arnold, J.G.; Van Liew, M.W.; Bingner, R.L.; Harmel, R.D.; Veith, T.L., (2007). Model evaluation guidelines for systematic quantification of accuracy in watershed simulations. Trans. Am. Soc. Agric. Biol. Eng., 50(3): 885-900 (**16 pages**).

Muhadi, N.A.; Abdullah, A.F.; Bejo, S.K.; Mahadi, M.R.; Mijic, A., (2020). The use of LiDAR-derived DEM in flood applications: A review. Remote Sens., 12(14), 1-20.

Najafi, S.; Salam, Z., (2016). Evaluating Prediction Accuracy for Collaborative Filtering Algorithms in Recommender Systems. Kth Royal Institute of Technology School of Computer Science and Communication, Stockholm, Sweden.

Ogania, J.L.; Puno, G.R.; Alivio, M.B.T.; Taylaran, J.M.G., (2019). Effect of digital elevation model's resolution in producing flood hazard maps. Global J. Environ. Sci. Manage., 5(1): 95-106 (**12 pages**).

Pinos, J.; Quesada-Roman, A., (2002). Flood Risk-Related Research Trends in Latin America and the Caribbean. Water, 14(1): 1-14 (**14 pages**).

Puno, G.R.; Amper, R.A.L.; Opiso, E.M.; Cipriano, J.A.B., (2019). Mapping and analysis of flood scenarios using numerical models and GIS techniques. Spatial Inf. Res., 28: 215-226 (**12 pages**).

Ronda, R.A., (2013). DOST project gets P2.4-B fund. ABS-CBN News, Manila.

Santillan, J.R.; Amora, A.M.; Makinano-Santillan, M.; Marqueso, J.T.; Cutamora, L.C.; Serviano, J.L.; Makinano, R.M., (2016). Assessing the impacts of flooding caused by extreme rainfall events through a combined geospatial and numerical modeling approach. Int. Arch. Photogramm. Remote Sens. Spatial Inf. Sci., XLI-B8: 1271–1278 (**8 pages**).

Sharma, M.; Paige, G.B.; Miller, S.N., (2010). DEM development from ground-based LiDAR data: a method to remove non-surface objects. Remote Sens., 2(11): 2629-2642 (**14 pages**).

Smith, L.C., (2002). Emerging applications of interferometric synthetic aperture radar (InSAR) in geomorphology and hydrology. Ann. Am. Assoc. Geogr., 92(3): 385-398 (**14 pages**).

Talisay, B.A.M.; Puno, G.R.; Amper, R.A.L., (2019). Flood hazard mapping in an urban area using combined hydrologic-hydraulic models and geospatial technologies. Global J. Environ. Sci. Manage., 5(2): 139-154 (**16 pages**).

Timbadiya, P.V.; Patel, P.L.; Porey, P.D., (2011). Calibration of HEC-RAS model on prediction of flood for lower Tapi river, India. J. Water Resour. Prot., 3(11): 805-811 (**7 pages**).

USACE, (1964). Hydrologic Engineering Center-Hydrologic Modeling System (HEC-HMS). The U.S. Army Corps of Engineers.

Wedajo, G.K., (2017). LiDAR DEM data for flood mapping and assessment; opportunities and challenges: A review. J. Remote Sens. Geog. Inf. Syst., 6(4): 1-4 (**4 pages**).

AUTHOR (S) BIOSKETCHES

PUNO, G.R., Ph.D., Professor, College of Forestry and Environmental Science, Central Mindanao University, Musuan, Bukidnon, Philippines.
- Email: grpuno@cmu.edu.ph
- ORCID: 0000-0002-7170-641X
- Web of Science ResearcherID: F-2553-2017
- Scopus Author ID: 56955824400
- Homepage: https://www.cmu.edu.ph/academic-units/forestry-and-environmental-science/

PUNO, R.C.C., M.Sc., Instructor, College of Forestry and Environmental Science, Central Mindanao University, Musuan, Maramag, Philippines
- Email: *rccpuno@cmu.edu.ph*
- ORCID: 0000-0001-7798-1335
- Web of Science ResearcherID: AAA-1038-2022
- Scopus Author ID: 57188870850
- Homepage: https://www.cmu.edu.ph/academic-units/forestry-and-environmental-science/

Maghuyop, I.V., M.Sc., Instructor, College of Forestry and Environmental Science, Central Mindanao University, Musuan, Maramag, Philippines
- Email: *ivmcfes@cmu.edu.ph*
- ORCID: 0000-0002-5035-8495
- Web of Science ResearcherID: AAA-2256-2022
- Scopus Author ID: NA

Homepage: https://www.cmu.edu.ph/academic-units/forestry-and-environmental-science/

HOW TO CITE THIS ARTICLE

Puno G.R., Puno R.C.C., Maghuyop I.V. (2022). Flood hazard simulation and mapping using digital elevation models with different resolutions. Global J. Environ. Sci.Manage., 8(3): 339-352.

DOI: 10.22034/gjesm.2022.03.04

url: https://www.gjesm.net/article_249008.html